A Biased Extended Kalman Filter for Indoor Localization of a Mobile Agent using Low-Cost IMU and UWB Wireless Sensor Network

A. Benini *, **A. Mancini** *, **A. Marinelli** *, **S. Longhi** *

* *Polytechnic University Of Marche, Department of Information Engineering (DII), Ancona, Italy (email: a.benini@univpm.it)*

Abstract: Indoor localization of mobile agents using wireless technologies is becoming very important in military and civil applications. This paper introduces an approach for the indoor localization of a mobile agent based on Ultra-WideBand technology using a Biased Extended Kalman Filter (EKF) as a possible technique to improve the localization. The proposed approach allows to use a low-cost IMU (inertial measurement unit) which performances are improved by a calibration procedure. The obtained results show that the filter allows to obtain better result in terms of localization due to the estimation of bias and scale factor.

Keywords: Indoor Localization, UWB, Low-cost IMU, RTLS, EKF

1. INTRODUCTION

Localization of mobile agents using wireless sensor network is becoming very attractive in many fields of applications such as logistics, military and security. Wireless sensor networks can be exploited successfully not only for communication among devices but also for localization purposes. IEEE 802.15.4a specifies two additional physical layers (PHYs): a PHY using ultra-wideband (UWB) and a PHY using chirp spread spectrum (CSS) both with a precision time-based ranging capability (Sahinoglu and Gezici (2006), Rohrig and Muller (2009), Sikora and Groza (2007), Krishnan et al. (2007)). The UWB PHY operates in three frequency bands: below 1 GHz, between 3 and 5 GHz, and between 6 and 10 GHz providing high ranging accuracy thanks to its large bandwidth. Furthermore, the UWB technology provides high data transfer, low power consumption, high spatial capacity of wireless data transmission and sophisticated usage of radio frequencies. UWB technology is based on sending and receiving carrier-less radio impulses using extremely accurate timing and it can be used in such applications where high bandwidth signals must be transmitted between devices. The CSS PHY is operating in 2.4 GHz ISM band and doesn't support ranging features. But the first 802.15.4a CSS chip (nanoLOC) developed by Nanotron has the ranging as additional (proprietary) function. It offers a unique solution for devices moving at high speeds because of its immunity to Doppler Effect and provides communicating at longer ranges. In (Sayed et al. (2005)) a review of existing ranging techniques is provided. RF Location System measures distances or angles between known points and an unknown position using several methods to obtain ranging measurements:

- Time-of-arrival of signal (ToA)
- Time-difference-of-arrival(TDoA)
- Angle-of-arrival(AoA)
- Received signal strength (RSSI)
- Time Of Flight (ToF)

An important drawback is that all these suffer from problems such us reflections, multipath and non-line-of-sight (NLOS) measurements: for communications, any signal path transfers useful information but for positioning only direct path signal carries useful information. This paper studies the indoor localization of a mobile agent using the UbiSense UWB Real-Time Localization System and low-cost IMU in conjunction with a Biased Extended Kalman Filter (BEKF). In order to improve the position accuracy also the bias and the scale factor for both accelerometer and gyroscope are considered. The paper is organized as follows. In the next section a concise overview of the UWB UbiSense Real-Time Localization System is provided. Section 3 deals with the low-cost IMU characterization focalizing the attention on bias and scale factor. In section 4 the mathematical model of the mobile agent is proposed. Then, in section 5 the BEKF algorithm is analyzed. In the last, some experimental results are discussed. This work extends our previous work (Benini et al. (2011)) that was based on indoor localization using CSS sensors; the limitation was the lower performances of CSS sensors compared to UWB sensors.

2. THE UWB UBISENSE REAL-TIME LOCALIZATION SYSTEM

The Ubisense RTLS is a precision measuring instrument. Each sensor contains an array of 4 UWB antennas used for receiving the radio pulses from the tags (device to localize). The sensors calculate the position of tags based on two different methodologies:

- Time Difference of Arrival (TDOA)
- Angle of Arrival (AOA)

This combination of methods provides a flexible system of localization in both indoor and outdoor environments, even in 3 dimensions. In addition the tag includes features for easy identification such as a motion detector sensor that activate the tag only when it moves (Corrales et al. (2008)). The sensors are connected to a controller PC (in which the localization server engine runs) through a POE Ethernet switch as shown in the following figure (Fig. 1):

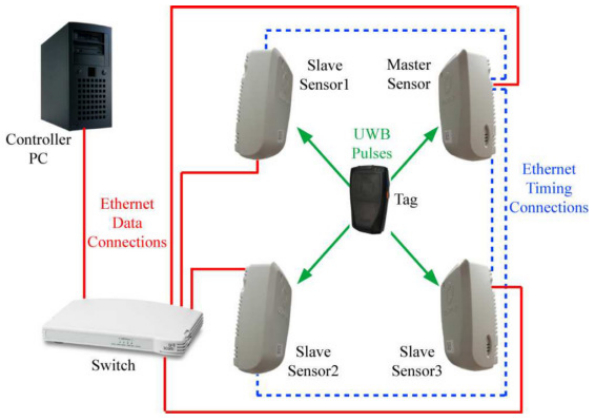

Fig. 1. The UbiSense system basic architecture

3. IMU CHARACTERIZATION

An Inertial Measurement Unit (IMU) is generally composed by two orthogonal sensor triads. A triad consists of three mono-axial accelerometers, the other consists of three mono-axial gyroscopes. The two triads are nominally parallel and the origin of the gyroscope is defined as the origin of the accelerometer triad. In recent years, solid state inertial sensors (MEMS) have found applications in many different fields, thanks especially to their low cost and very small size (De Agostino et al. (2010)). But low cost sensors are generally characterized by poor performances. The most important drawbacks of a MEMS IMU are *bias* and *scale factor* (Kau et al. (2000); Hung et al. (1989); Hyun et al. (2009); Hulsing (1998a,b)). So, in order to obtain good positioning accuracies, it is necessary to analyze deeply the behaviour of the sensors and implements special test calibrations, both in static and kinematic conditions (Feng et al. (1994)).

The acceleration among an axis can be expressed by the following relationship (eq. 1), in which we don't consider the thermal drift:

$$\ddot{z_a} = \ddot{z} + g + \epsilon_a + S_a g + v \tag{1}$$

where

- $\ddot{z}_a$ is the measured acceleration in output to the sensor
- $\ddot{z}$ is the true values of the acceleration (at the considered point)
- g is the gravity acceleration
- ϵ_a is the bias
- S_a is the scale factor
- v is the noise

The ϵ_a and S_a coefficient are supposed constant over long period. For the scale factor estimation, the *six-position face test* has been used (De Bento et al. (2010); De Agostino et al. (2010); Titterton and Weston (2004); Hung et al. (1989)). We used the InvenSense MPU 6050 (Fig. 2) whose specifications are reported in Table 1.

Specifications	Accelerometers	Gyroscopes
Range	$\pm 2g$	$\pm 250°/s$
Bias	$\pm 50mg$	$\pm 20°/s$
Non-ortogonality	$\pm 2\%$	$\pm 2\%$
Random Walk	$400\mu G/\sqrt{Hz}$	$0.005°/s/\sqrt{Hz}$

Table 1. InvenSense MPU6050 Specifications

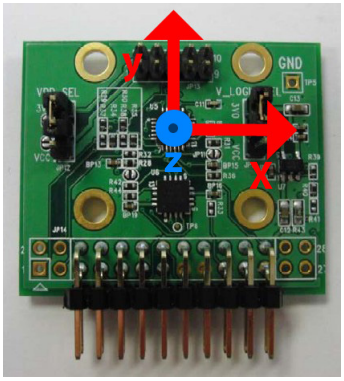

Fig. 2. The InvenSense®MPU-6050 IMU with Axis references

3.1 The Scale Factor estimation

The scale factor can be described by the following relationship (eq. 2):

$$S_a = \frac{\ddot{z}_{down} - \ddot{z}_{up} - 2g}{2g} \tag{2}$$

where $\ddot{z}_{down}$ and $\ddot{z}_{up}$ are respectively two static measurement carried out holding the z axis of the accelerometer downward and upward. A similar mechanism is applied in order to estimate the scale factor among the other two axis.

3.2 The bias estimation

In Barshan and Durrant-Whyte (1995, 1993), for the bias estimation ϵ, the following non-linear parametric model has been used (eq. 3):

$$\epsilon(t) = C_1(1 - e^{-\frac{t}{T}}) + C_2 \tag{3}$$

with parameters C_1, C_2 and T to be tuned by mean of long static measurement. The parametrized model of equation 3 can be expressed as follows (eq. 4):

$$\epsilon_{k+1} = \frac{T}{T + T_c}\epsilon_k + \frac{T_c}{T_c + T}(C_1 + C_2) \tag{4}$$

with the initial condition

$$\epsilon(0) = C_2 \tag{5}$$

Equation 4 is also used for the determination of the bias of the gyroscope. For parameters estimation, a data acquisition of 2 hours @200Hz (maximum data rate for InvenSense MPU 6050) has been carried out. Using the Iterative Levenberg−Marquardt Least Squares Fit method, resulting parameters are expressed in the following table (Table 2).

	C_1	C_2	T
a_x	$0.7562 m/s^2$	$-0.8255 m/s^2$	$0.3042\ s$
a_y	$0.0514 m/s^2$	$-0.0451 m/s^2$	$0.7573\ s$
ω_z	$1.138°/s$	$16.41°/s$	$1.565\ s$

Table 2. Drift model parameters for Inertial Sensor using Barshan-Durrant White procedure

4. THE MATHEMATICAL MODEL

Starting from the physical laws that describes the uniform change of speed of a point P in one dimension:

$$p(t) = p(t-1) + \Delta p(t) = p(t-1) + \iint_{t-1}^{t} \alpha(\tau)\, \mathrm{d}\tau \quad (6)$$

the two-dimensional version can be expressed as:

$$p_x = \iint_{t-1}^{t} \alpha_x(\tau) cos(\theta(\tau)) - \alpha_y(\tau) sin(\theta(\tau))\, \mathrm{d}\tau \quad (7)$$

$$p_y = \iint_{t-1}^{t} \alpha_x(\tau) sin(\theta(\tau)) + \alpha_y(\tau) cos(\theta(\tau))\, \mathrm{d}\tau \quad (8)$$

or, in matrix form:

$$\begin{bmatrix} p_x \\ p_y \end{bmatrix} = \iint \begin{bmatrix} cos(\theta(\tau)) & -sin(\theta(\tau)) \\ sin(\theta(\tau)) & cos(\theta(\tau)) \end{bmatrix} \begin{bmatrix} a_x(\tau) \\ a_y(\tau) \end{bmatrix} \mathrm{d}\tau \quad (9)$$

where

$$\begin{bmatrix} cos(\theta(\tau)) & -sin(\theta(\tau)) \\ sin(\theta(\tau)) & cos(\theta(\tau)) \end{bmatrix} = R \quad (10)$$

is the rotational matrix in two dimensions. At discrete time, equations 7 can be expressed in the following way:

$$x_{k+1} = x_k + \frac{{T_c}^2}{2} a_{xk} cos(\theta_k) - \frac{{T_c}^2}{2} a_{yk} sin(\theta_k) \quad (11)$$

$$y_{k+1} = y_k + \frac{{T_c}^2}{2} a_{xk} sin(\theta_k) + \frac{{T_c}^2}{2} a_{yk} cos(\theta_k) \quad (12)$$

where θ_k is the angle among the z axis (azimuth angle, see Fig. 3) equals to:

$$\theta_{k+1} = \theta_k + T_c \omega_k \quad (13)$$

and Tc is the sample time ($Tc = 0.1s$). Using equation 2 and 4, we can include the bias and scale factor in the accelerometer model

$$a_{k+1} = a_k(1 + S_{ak} sign(a_k)) - \epsilon_{ak} \quad (14)$$

Because also the gyroscope is affected by bias, the angular velocity can be expressed as

$$\omega_{k+1} = \omega_k - \epsilon_{\omega k} \quad (15)$$

After these considerations, the state vector of the model is expressed as follows:

$$\mathbf{x}_k = [x_k\ a_{xk}\ \epsilon_{x_k}\ y_k\ a_{yk}\ \epsilon_{y_k}\ \theta_k\ \omega_k\ \epsilon_{\omega_k}] \quad (16)$$

5. THE EXTENDED KALMAN FILTER

Data provided by IMU and ranging sensors are combined by a sensor-fusion algorithm based on Extended Kalman Filter (EKF). The following flow chart shows how the sensor fusion algorithm works (Fig. 4).

In the Extended Kalman Filter, the state transition and observation model need not be linear functions of the state but may be differentiable functions instead (Welch and Bishop (2001)). Let's define the dynamic equation and the measurement equation respectively as:

$$\tilde{\mathbf{x}}_{k+1} = f(\hat{\mathbf{x}}_k, \mathbf{u}_k, \mathbf{w}_k) \quad (17)$$

$$\tilde{\mathbf{y}}_{k+1} = h(\tilde{\mathbf{x}}_{k+1}, \mathbf{v}_{k+1}) \quad (18)$$

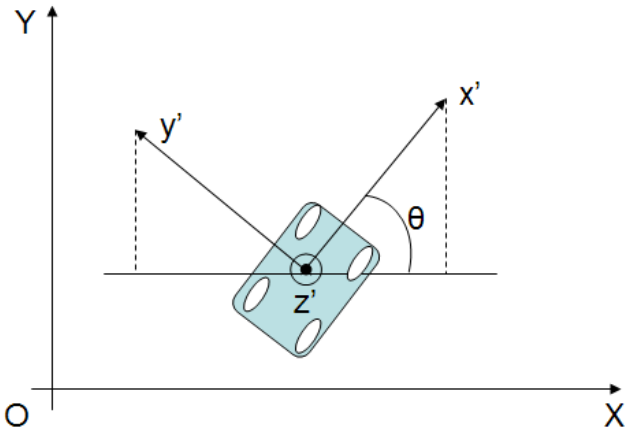

Fig. 3. The Mobile agent with the body coordinates system used

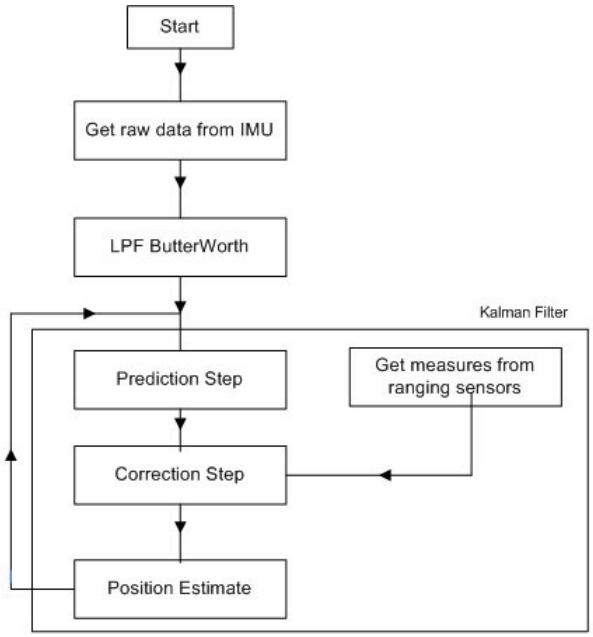

Fig. 4. Flow chart of the sensor fusion algorithm

where $\tilde{x}_k$ and $\tilde{y}_k$ denote the approximated *a priori* state and observation while $\hat{x}_k$ the *a posteriori* state estimation at the previous step. The process function f can be expressed as a linear function

$$\mathbf{x}_{k+1} = A\mathbf{x}_k + B\mathbf{u}_k + \mathbf{w}_k \quad (19)$$

where

$$A(k) = \frac{\partial f(\mathbf{x}(k), u(k), w(k)}{\partial x}\Big|_{\hat{\mathbf{x}}(k)} = \quad (20)$$

$$= \begin{bmatrix} \frac{\partial f_1}{\partial x_1}\Big|_{\hat{\mathbf{x}}(k)} & \cdots & \frac{\partial f_1}{\partial x_n}\Big|_{\hat{\mathbf{x}}(k)} \\ \vdots & \ddots & \vdots \\ \frac{\partial f_n}{\partial x_1}\Big|_{\hat{\mathbf{x}}(k)} & \cdots & \frac{\partial f_n}{\partial x_n}\Big|_{\hat{\mathbf{x}}(k)} \end{bmatrix} \quad (21)$$

which gives:

$$A = \begin{bmatrix} 1 & a_{12} & 0 & 0 & a_{15} & 0 & a_{17} & 0 & 0 \\ 0 & a_{22} & -1 & 0 & 0 & 0 & 0 & 0 & 0 \\ 0 & 0 & \frac{T_{a_x}}{T_{a_x}+T_c} & 0 & 0 & 0 & 0 & 0 & 0 \\ 0 & a_{42} & 0 & 1 & a_{45} & 0 & a_{47} & 0 & 0 \\ 0 & 0 & 0 & 0 & a_{55} & -1 & 0 & 0 & 0 \\ 0 & 0 & 0 & 0 & 0 & \frac{T_{a_y}}{T_{a_y}+T_c} & 0 & 0 & 0 \\ 0 & 0 & 0 & 0 & 0 & 0 & 1 & T_c & 0 \\ 0 & 0 & 0 & 0 & 0 & 0 & 0 & 0 & -1 \\ 0 & 0 & 0 & 0 & 0 & 0 & 0 & 0 & \frac{T_{\omega_z}}{T_{\omega_z}+T_c} \end{bmatrix} \tag{22}$$

where

$$a_{12} = \frac{T_c^2}{2} cos\theta(k) \tag{23}$$

$$a_{15} = -\frac{T_c^2}{2} sin\theta(k) \tag{24}$$

$$a_{17} = -\frac{T_c^2}{2} a_x(k) sin\theta(k) - \frac{T_c^2}{2} a_y(k) cos\theta(k) \tag{25}$$

$$a_{22} = 1 + (K_{ax} \cdot sign(a_x(k)) \tag{26}$$

$$a_{42} = \frac{T_c^2}{2} sin\theta(k) \tag{27}$$

$$a_{45} = \frac{T_c^2}{2} cos\theta(k) \tag{28}$$

$$a_{47} = \frac{T_c^2}{2} a_x(k) cos\theta(k) - \frac{T_c^2}{2} a_y(k) sin\theta(k) \tag{29}$$

$$a_{55} = 1 + (K_{ay} \cdot sign(a_y(k)) \tag{30}$$

and the scale factors are, respectively $K_{ax} = 0.17$ and $K_{ay} = 0.16$. Assuming that in the IMU noise associated with each sensor is uncorrelated with that of the other, the covariance matrix of process noise Q will be diagonal to blocks (Bar-Shalom (1987)):

$$Q = E\{w(k)w^T(k)\} = \begin{bmatrix} Q_{a_x} & 0 & 0 \\ 0 & Q_{a_y} & 0 \\ 0 & 0 & Q_{\omega_z} \end{bmatrix} \tag{31}$$

where:

$$Q_{a_i} = \begin{bmatrix} \frac{T_c^5}{20}\sigma_i^2 & \frac{T_c^3}{6}\sigma_i^2 & 0 \\ \frac{T_c^3}{6}\sigma_i^2 & T_c\sigma_i^2 & 0 \\ 0 & 0 & T_c\sigma_{a_i}^2 \end{bmatrix} \tag{32}$$

$$Q_{\omega_z} = \begin{bmatrix} \frac{T_c^3}{3}\sigma_{\omega_z}^2 & \frac{T_c^2}{2}\sigma_{\omega_z}^2 & 0 \\ \frac{T_c^2}{2}\sigma_{\omega_z}^2 & T_c\sigma_{\omega_z}^2 & 0 \\ 0 & 0 & T_c\sigma_{\omega}^2 \end{bmatrix} \tag{33}$$

where σ_x, σ_y and σ_ω have been determined experimentally in the characterization phase of the inertial sensor, while σ_{ai} and $\sigma\omega$ are the standard deviations of the residuals fitting.

Sensor measurements at time k are modeled in a Kalman Filter by the following equation (measurement model):

$$\mathbf{z}_k = H\mathbf{x}_k + \mathbf{v}_k \tag{34}$$

Because the UbiSense UWB system provides only the (x,y,z) coordinate of the estimated position of the tag, the H matrix is built in the following way:

$$H = \begin{bmatrix} 1 & 0 & 0 & 0 & 0 & 0 & 0 & 0 & 0 \\ 0 & 0 & 0 & 1 & 0 & 0 & 0 & 0 & 0 \end{bmatrix} \tag{35}$$

6. EXPERIMENTAL RESULTS

In this section we present the results of some tests carried out in indoor environment (Fig. 5). The reason of this choice is for the performances evaluations of the algorithm even in presence of multipath. The 2-D Cartesian coordinates of anchors have the following values (expressed in meters):

$$\begin{aligned} \mathbf{A}_1 &= [0.18 \quad 0.79]^T \\ \mathbf{A}_2 &= [1.79 \quad 8.107]^T \\ \mathbf{A}_3 &= [7.31 \quad 9.28]^T \\ \mathbf{A}_4 &= [4.62 \quad 0.23]^T \end{aligned} \tag{36}$$

The initial position of the mobile agent is $[3.4 \quad 2.4]^T m$.

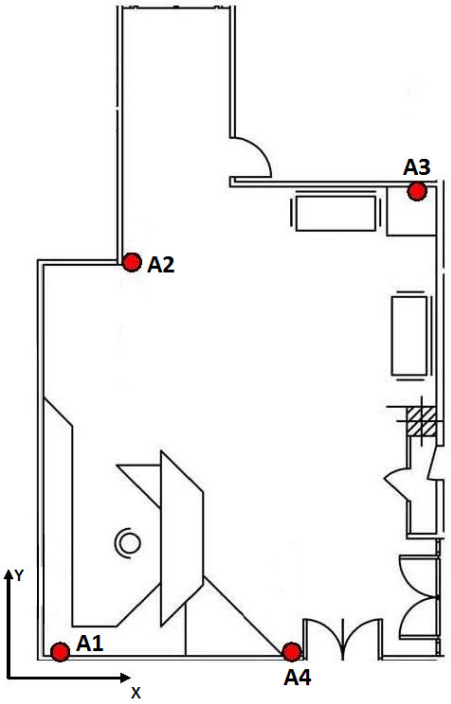

Fig. 5. Map of the indoor environment

The speed of the mobile agent is set to 1 m/s. While the mobile agent moves along the path, the UWB tag node measures ranging from the four anchors and then a trilateration of (x,y) position is provided to the mobile agent from the UbiSense Location Engine.

The obtained results (see Fig. 6,7) show that the filter allows to obtain better result in terms of localization due to the estimation of bias and scale factor. The error amplitude is less than the UbiSense resolution ($\sim 15cm$) and the algorithm provides a better state estimation also when the mobile agent is standing in a fixed point (Fig. 8).

7. CONCLUSION

In this paper a Biased Extended Kalman filter for indoor localization using a 802.15.4a Wireless Network was presented. The calibration procedure for MEMS is a critical

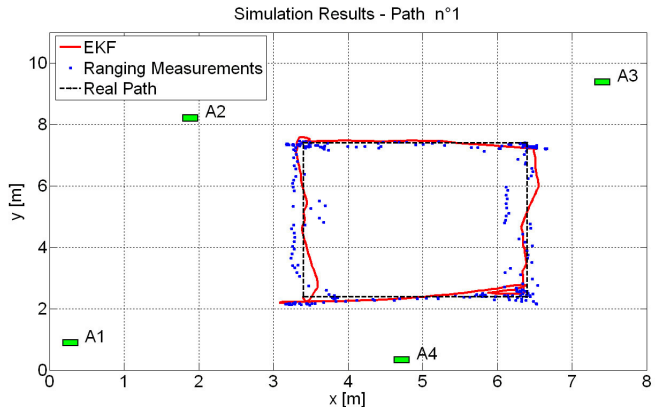

Fig. 6. Experimental results in indoor environment - Test $n°1$

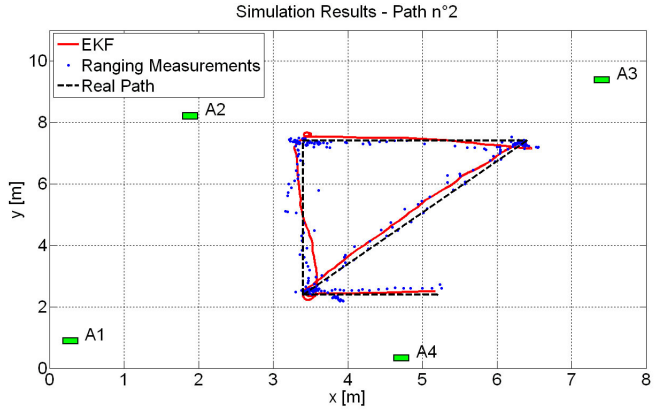

Fig. 7. Experimental results in indoor environment - Test $n°2$

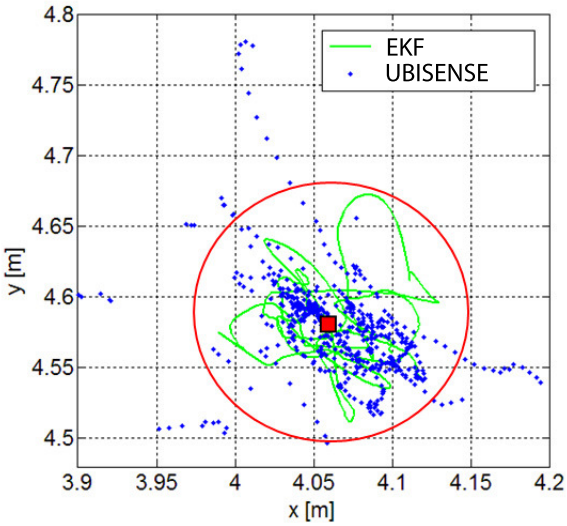

Fig. 8. Experimental results with the mobile agent (red square) standing in a fixed point

aspect that needs to be carried out in order to improve the a priori state estimation. The obtained results reinforce the necessity of integrate additional sensors to obtain better results in terms of accuracy and precision. In case of indoor environments the integration of Laser Range Finder or camera could significantly improve the overall performance (Cesetti et al. (2010); Ascani et al. (2008)). Future works will be steered to extend the set of sensors integrating visual information based on SIFT/SURF feature detection also for Simultaneous Localization and Mapping (Khoshelham et al. (2010)) in multi-robot scenarios (Mancini et al. (2009)) and to evaluate this technology also for the pedestrian localization.

ACKNOWLEDGEMENTS

This work is developed in the context of ARTEMIS-JU EU Project R3-COP. In particular the authors would like to thank Mauro Montanari and Riccardo Minutolo (Thales Italia S.p.A) for their support.

REFERENCES

Ascani, A., Frontoni, E., Mancini, A., and Zingaretti, P. (2008). Feature group matching for appearance-based localization. In *Intelligent Robots and Systems, 2008. IROS 2008. IEEE/RSJ International Conference on*, 3933 –3938. doi:10.1109/IROS.2008.4651023.

Bar-Shalom, Y. (1987). *Tracking and data association*. Academic Press Professional, Inc., San Diego, CA, USA.

Barshan, B. and Durrant-Whyte, H. (1993). An inertial navigation system for a mobile robot. In *Intelligent Robots and Systems '93, IROS '93. Proceedings of the 1993 IEEE/RSJ International Conference on*, volume 3, 2243 –2248 vol.3. doi:10.1109/IROS.1993.583939.

Barshan, B. and Durrant-Whyte, H. (1995). Inertial navigation systems for mobile robots. *Robotics and Automation, IEEE Transactions on*, 11(3), 328 –342. doi:10.1109/70.388775.

Benini, A., Mancini, A., Frontoni, E., Zingaretti, P., and Longhi, S. (2011). Adaptive extended kalman filter for indoor/outdoor localization using a 802.15.4a wireless network. In *European Conference on Mobile Robots, 2011. ECMR 2011.*

Cesetti, A., Frontoni, E., Mancini, A., Zingaretti, P., and Longhi, S. (2010). A vision-based guidance system for uav navigation and safe landing using natural landmarks. *Journal of Intelligent Robotic Systems*, 57, 233–257. URL `http://dx.doi.org/10.1007/s10846-009-9373-3`. 10.1007/s10846-009-9373-3.

Corrales, J.A., Candelas, F.A., and Torres, F. (2008). Hybrid tracking of human operators using imu/uwb data fusion by a kalman filter. In *Proceedings of the 3rd ACM/IEEE international conference on Human robot interaction*, HRI '08, 193–200. ACM, New York, NY, USA. doi:http://doi.acm.org/10.1145/1349822.1349848. URL `http://doi.acm.org/10.1145/1349822.1349848`.

De Agostino, M., Manzino, A.M., and Piras, M. (2010). Performances comparison of different mems-based imus. In *Position Location and Navigation Symposium (PLANS), 2010 IEEE/ION*, 187 –201. doi:10.1109/PLANS.2010.5507128.

De Bento, M., Eissfeller, B., and Machado, F. (2010). How to deal with low performance imus in an integrated navigation system: Step by step. In *Satellite Navigation Technologies and European Workshop on GNSS Signals and Signal Processing (NAVITEC), 2010 5th ESA Workshop on*, 1 –10. doi:10.1109/NAVITEC.2010.5708042.

Feng, L., Everett, H., Borenstein, J., of Michigan., U., Laboratory., O.R.N., and States., U. (1994). *"Where am I?" : sensors and methods for autonomous mobile robot positioning. Vol. 3 / by L. Feng, J. Borenstein and H.R. Everett ; edited and compiled by J. Borenstien.* University of Michigan, Michigan :.

Hulsing, R. (1998a). Mems inertial rate and acceleration sensor. *Aerospace and Electronic Systems Magazine, IEEE*, 13(11), 17 –23. doi:10.1109/62.730613.

Hulsing, R. (1998b). Mems inertial rate and acceleration sensor. In *Position Location and Navigation Symposium, IEEE 1998*, 169 –176. doi:10.1109/PLANS.1998.670038.

Hung, J., Thacher, J., and White, H. (1989). Calibration of accelerometer triad of an imu with drifting z -accelerometer bias. In *Aerospace and Electronics Conference, 1989. NAECON 1989., Proceedings of the IEEE 1989 National*, 153 –158 vol.1. doi:10.1109/NAECON.1989.40206.

Hyun, D., Yang, H.S., Yuk, G.H., and Park, H.S. (2009). A dead reckoning sensor system and a tracking algorithm for mobile robots. In *Mechatronics, 2009. ICM 2009. IEEE International Conference on*, 1 –6. doi:10.1109/ICMECH.2009.4957155.

Kau, S., Boutelle, J., and Lawdermilt, L. (2000). Accelerometer input axis angular acceleration sensitivity. In *Position Location and Navigation Symposium, IEEE 2000*, 449 –456. doi:10.1109/PLANS.2000.838338.

Khoshelham, K., Nardinocchi, C., Frontoni, E., Mancini, A., and Zingaretti, P. (2010). Performance evaluation of automated approaches to building detection in multi-source aerial data. *ISPRS Journal of Photogrammetry and Remote Sensing*, 65(1), 123 – 133. doi:10.1016/j.isprsjprs.2009.09.005. URL `http://www.sciencedirect.com/science/article/pii/S0924271609001191`.

Krishnan, S., Sharma, P., Guoping, Z., and Woon, O.H. (2007). A uwb based localization system for indoor robot navigation. In *IEEE International Conference on Ultra-Wideband, 2007. ICUWB 2007.*, 77 –82. doi:10.1109/ICUWB.2007.4380919.

Mancini, A., Cesetti, A., Iual, A., Frontoni, E., Zingaretti, P., and Longhi, S. (2009). A framework for simulation and testing of uavs in cooperative scenarios. *Journal of Intelligent Robotic Systems*, 54, 307–329. URL `http://dx.doi.org/10.1007/s10846-008-9268-8`. 10.1007/s10846-008-9268-8.

Rohrig, C. and Muller, M. (2009). Indoor location tracking in non-line-of-sight environments using a ieee 802.15.4a wireless network. In *IEEE/RSJ International Conference on Intelligent Robots and Systems, 2009. IROS 2009*, 552 –557. doi:10.1109/IROS.2009.5354747.

Sahinoglu, Z. and Gezici, S. (2006). Ranging in the ieee 802.15.4a standard. In *IEEE Annual Wireless and Microwave Technology Conference, 2006. WAMICON '06.*, 1 –5. doi:10.1109/WAMICON.2006.351897.

Sayed, A., Tarighat, A., and Khajehnouri, N. (2005). Network-based wireless location: challenges faced in developing techniques for accurate wireless location information. *Signal Processing Magazine, IEEE*, 22(4), 24 – 40. doi:10.1109/MSP.2005.1458275.

Sikora, A. and Groza, V. (2007). Fields tests for ranging and localization with time-of-flight-measurements using chirp spread spectrum rf-devices. In *IEEE Instrumentation and Measurement Technology Conference Proceedings, 2007. IMTC 2007.*, 1 –6. doi:10.1109/IMTC.2007.379151.

Titterton, D. and Weston, J. (2004). *Strapdown Inertial Navigation Technology.* The American Institute of Aeronautics and Astronautics, second edition.

Welch, G. and Bishop, G. (2001). An introduction to the kalman filter. *Design*, 7(1), 1–16. URL `http://citeseerx.ist.psu.edu/viewdoc/download?doi=10.1.1.79.6578&rep=rep1&type=pdf`.